Decreased RyR2 refractoriness determines myocardial synchronization of aberrant Ca^{2+} release in a genetic model of arrhythmia

Lucia Brunello[a], Jessica L. Slabaugh[b], Przemysław B. Radwański[a], Hsiang-Ting Ho[a], Andriy E. Belevych[a], Qing Lou[a], Haiyan Chen[c], Carlo Napolitano[d], Francesco Lodola[d], Silvia G. Priori[d], Vadim V. Fedorov[b], Pompeo Volpe[e], Michael Fill[c], Paul M. L. Janssen[b,1], and Sándor Györke[a,1]

[a]D. Davis Heart and Lung Research Institute and [b]Department of Physiology and Cell Biology, College of Medicine, The Ohio State University, Columbus, OH 43210; [c]Department of Molecular Biophysics and Physiology, Section of Cellular Signaling, Rush University Medical Center, Chicago, IL 60612; [d]Divisione di Cardiologia, Instituto di Ricovero e Cura a Carattere Scientifico Fondazione Salvatore Maugeri, 27100 Pavia, Italy; and [e]Department of Biomedical Sciences, University of Padova, 35121 Padova, Italy

Edited by Gerhard Meissner, University of North Carolina at Chapel Hill, Chapel Hill, NC, and accepted by the Editorial Board May 6, 2013 (received for review January 2, 2013)

Dysregulated intracellular Ca^{2+} signaling is implicated in a variety of cardiac arrhythmias, including catecholaminergic polymorphic ventricular tachycardia. Spontaneous diastolic Ca^{2+} release (DCR) can induce arrhythmogenic plasma membrane depolarizations, although the mechanism responsible for DCR synchronization among adjacent myocytes required for ectopic activity remains unclear. We investigated the synchronization mechanism(s) of DCR underlying untimely action potentials and diastolic contractions (DCs) in a catecholaminergic polymorphic ventricular tachycardia mouse model with a mutation in cardiac calsequestrin. We used a combination of different approaches including single ryanodine receptor channel recording, optical imaging (Ca^{2+} and membrane potential), and contractile force measurements in ventricular myocytes and intact cardiac muscles. We demonstrate that DCR occurs in a temporally and spatially uniform manner in both myocytes and intact myocardial tissue isolated from cardiac calsequestrin mutation mice. Such synchronized DCR events give rise to triggered electrical activity that results in synchronous DCs in the myocardium. Importantly, we establish that synchronization of DCR is a result of a combination of abbreviated ryanodine receptor channel refractoriness and the preceding synchronous stimulated Ca^{2+} release/reuptake dynamics. Our study reveals how aberrant DCR events can become synchronized in the intact myocardium, leading to triggered activity and the resultant DCs in the settings of a cardiac rhythm disorder.

calcium-induced calcium release | luminal calcium | RyR2 deactivation | sarcoplasmic reticulum

Cardiac arrhythmias are the most common and lethal cardiac diseases, accounting for around 450,000 deaths annually in the United States alone (1). The majority of these deaths are caused by irregular ectopic beats that lead to ventricular tachycardia and fibrillation. The normal rhythmic beating of the heart is maintained by the cross-talk between the action potential (AP) and self-regenerating Ca^{2+}-induced Ca^{2+} release (CICR), where Ca^{2+} entry during the cardiac AP ignites CICR. The CICR is mediated by the ryanodine receptor (RyR2) on the sarcoplasmic reticulum (SR) and contributes to the global intracellular Ca^{2+} transient that drives cardiomyocyte contraction. Following Ca^{2+} release and contraction, relaxation ensues as Ca^{2+} is resequestered back into the SR by the SR Ca^{2+} pump (2). Importantly for normal Ca^{2+} cycling, the SR becomes refractory after each systolic Ca^{2+} release, thereby preventing spontaneous reactivation of CICR during the diastolic period (3–5). This temporal restraint of Ca^{2+} signaling is thought to be a consequence of the local decrease in intra-SR Ca^{2+} that in turn can inhibit CICR either by reducing RyR2 Ca^{2+} efflux (6) and/or by deactivating RyR2s via a mechanism that involves the SR Ca^{2+} binding protein calsequestrin 2 (CASQ2) (7–9).

In various disease settings, aberrant diastolic Ca^{2+} release (DCR) from the SR gives rise to arrhythmic ectopic activity (10–14). The pathologic link between diastolic dysregulated Ca^{2+} release and arrhythmia is particularly evident in catecholaminergic polymorphic ventricular tachycardia (CPVT), a familial form of arrhythmia caused by mutations in the components of the RyR2 complex, including RyR2 and CASQ2 (15, 16). In myocytes harboring CPVT-associated CASQ2 mutations, altered CASQ2-dependent RyR2 modulation predisposes the SR to spontaneous DCR. DCR occurs in the form of waves of self-propagating CICR. These waves result in Ca^{2+}-dependent depolarizing currents generated by the electrogenic Na^+/Ca^{2+} exchanger activity on the cell membrane giving rise to delayed afterdepolarizations (DADs) and consequently to triggered arrhythmias (17–19).

Despite the fact that the mechanisms of triggered arrhythmias have been well established on the cellular level, the relationship between abnormal myocyte Ca^{2+} cycling and focal excitation at the tissue level remains poorly understood. A key unresolved question is how spontaneous Ca^{2+} release in individual myocytes can cause a sufficiently large membrane depolarization to elicit an ectopic event across the whole of myocardium, particularly because a local depolarizing current is expected to be absorbed by the electrically connected neighboring myocytes serving as current sinks (20). Consequently, it has been suggested that ectopic activity, rather than arising in individual ventricular myocytes, originates in the Purkinje system, which has a smaller source-sink mismatch relative to the 3D ventricular network (21). Thus, there is uncertainty whether and how focally activated arrhythmias such as CPVT can originate in the ventricular myocardium. Here, our focus is a murine model of CPVT with a point mutation in CASQ2 ($CASQ2^{R33Q}$) that causes an impairment of store-dependent RyR2 deactivation (22). We demonstrate that this impairment alters refractoriness of Ca^{2+} release, which in turn provides a mechanism for synchronization of DCR, DADs, and diastolic contractions (DCs) across intact myocardium. Importantly, our study provides a conceptual framework in which

Author contributions: L.B., P.B.R., A.E.B., P.V., M.F., P.M.L.J., and S.G. designed research; L.B., J.L.S., P.B.R., H.-T.H., A.E.B., Q.L., and H.C. performed research; Q.L., C.N., F.L., S.G.P., V.V.F., and P.M.L.J. contributed new reagents/analytic tools; L.B., J.L.S., P.B.R., A.E.B., Q.L., and H.C. analyzed data; and L.B., P.B.R., P.V., M.F., P.M.L.J., and S.G. wrote the paper.

The authors declare no conflict of interest.

This article is a PNAS Direct Submission. G.M. is a guest editor invited by the Editorial Board.

Freely available online through the PNAS open access option.

[1]To whom correspondence may be addressed. E-mail: Sandor.Gyorke@osumc.edu or janssen.10@osu.edu.

This article contains supporting information online at www.pnas.org/lookup/suppl/doi:10.1073/pnas.1300052110/-/DCSupplemental.

store-dependent RyR2 deactivation on the cellular level serves as a substrate for triggered arrhythmias at the whole heart level.

Results

Spontaneous Ca^{2+} Release Is Associated with Reduced RyR2 Refractoriness in $CASQ2^{R33Q}$ Myocytes. Myocytes isolated from WT and $CASQ2^{R33Q}$ hearts were paced at 1 Hz in the presence of the β-adrenergic agonist isoproterenol (ISO, 100 nM, Fig. 1*A*). Under these conditions, DCR (waves and/or wavelets) occurred at a frequency of 0.24 ± 0.06 events per cycle in $CASQ2^{R33Q}$ myocytes, which was significantly higher than those in WT myocytes (0.03 ± 0.01 events per cycle, Fig. 1*C*). The few DCRs observed in WT myocytes were randomly distributed through diastole. In contrast, DCRs in $CASQ2^{R33Q}$ cells had a high probability of occurrence around three distinct time points consistent with the development of up to three DCRs during the diastolic period. The distribution of DCRs reveals a well-defined periodicity with a fixed interrelease interval of ∼260 ms (Fig. 1*D*). Of note, the occurrence of DCR displayed a clear rate dependency such that the number of events per cycle decreased and their distribution narrowed at faster pacing rates (Fig. S1).

To gain further insights into the mechanisms of DCR, we examined more closely the distribution of the latencies to the first DCR. In $CASQ2^{R33Q}$ myocytes, the histogram after an initial time lag of ∼200 ms showed a sharp peak followed by a gradual, close to exponential decay (Fig. 1*E*). As demonstrated by Maltsev et al. (23) in pacemaker cells with robust Ca^{2+} oscillations, the high synchronicity of spontaneous firing of release sites is attributable to synchronization of refractory periods. Thus, the 200-ms time lag before the first DCR in $CASQ2^{R33Q}$ myocytes provides a metric consistent with the RyR2 refractory period. In contrast, DCRs in WT myocytes were less frequent and occurred more randomly, with a median time of onset occurring at 751 ms, which was distinctly longer relative to $CASQ2^{R33Q}$ myocytes (Fig. 1*F*). Based on previous work by Maltsev et al. (23), the increased synchronicity of release events in $CASQ2^{R33Q}$ cells could be ascribed to either an increased magnitude of Ca^{2+} release through RyR2s and/or altered refractory properties of RyR2s (facilitating CICR). Because the amplitude of Ca^{2+} transients decreased in $CASQ2^{R33Q}$ compared with WT myocytes (Fig. 1*B*), an alteration in refractoriness of release is the likely factor behind the increased synchronicity of DCR during CPVT.

To more closely assess the refractory properties of Ca^{2+} signaling in $CASQ2^{R33Q}$ and WT myocytes, we measured the restitution of SR Ca^{2+} release using an established S1-S2 protocol in which the first stimulus is followed by a second one after a varying time interval (Fig. 2*A*). This protocol revealed that the restitution of Ca^{2+} release, as evidenced by the rate of recovery of Ca^{2+} transient amplitude, was significantly accelerated in $CASQ2^{R33Q}$ myocytes, consistent with impaired Ca^{2+} signaling refractoriness in these cells (Fig. 2*B*). Furthermore, to examine whether these differences in recovery of Ca^{2+} release are caused by potential alterations in Ca^{2+} currents (I_{Ca}), we performed measurements of I_{Ca} restitution in patch-clamped myocytes following the same S1-S2 protocol as mentioned previously. The recovery of the peak I_{Ca} was similar in both myocyte groups, suggesting that I_{Ca} is unlikely to underlie the differences in release restitution (Fig. S2).

To examine whether the altered Ca^{2+} signaling in $CASQ2^{R33Q}$ myocytes was associated with altered RyR2 function, we performed single-channel measurements in RyR2s incorporated into lipid bilayers. Previously, we demonstrated that the R33Q CASQ2 variant lacks the ability of its WT counterpart to inhibit RyR2 at low luminal Ca^{2+} (20 μM) (24). Here we examined whether altered modulation of RyR2 activity by $CASQ2^{R33Q}$ is present at a higher, near-diastolic luminal [Ca^{2+}] (1 mM). Indeed, at this Ca^{2+}, RyR2 open probability (Po) was significantly higher, whereas the mean closed time (MCT) was significantly shorter in $CASQ2^{R33Q}$ RyR2s compared with WT channels (Fig. 2 *C–F*). Consistent with these results in single RyR2s, diastolic Ca^{2+} sparks occurred more frequently in $CASQ2^{R33Q}$ than in WT myocytes (4.4 ± 1.1 vs. 2.5 ± 0.3 0.1 $mm^{-1}{\cdot}s^{-1}$; n = 74–621 events; $P < 0.05$). Collectively, these data suggest that impaired refractory behavior of individual RyR2s leads to temporally aligned DCR in $CASQ2^{R33Q}$ myocytes.

Highly Synchronized DCs in Intact $CASQ2^{R33Q}$ Muscle. To test whether the temporal synchronization of spontaneous DCR in myocytes isolated from $CASQ2^{R33Q}$ mice gives rise to synchronous DCs in cardiac muscle, we performed force measurements in multicellular papillary muscle and trabeculae preparations. Muscles from WT and $CASQ2^{R33Q}$ mice were electrically paced at 1 Hz, and mechanical force was measured before and after exposure to ISO (Fig. 3*A*). Under baseline conditions (upper traces), WT and $CASQ2^{R33Q}$ muscles exhibited regular twitches of similar amplitude and time course (Fig. 3 *A*, *E*, and *F*). Exposure to ISO (30–300 nM; lower traces in Fig. 3*A*) effectively tripled the frequency of contractions because of the occurrence of unprovoked diastolic events in $CASQ2^{R33Q}$ but not in WT muscles. As expected, ISO significantly increased average twitch force amplitude in WT muscles. Interestingly, the average twitch force amplitude at the peak ISO effect remained unchanged in $CASQ2^{R33Q}$ muscles. This is mainly due to the increased DCR frequency depleting the SR Ca^{2+} store (Fig. 3*E*). Superimposed traces from different $CASQ2^{R33Q}$ muscles challenged with ISO are shown in Fig. 3*B*. As in myocyte experiments, the DCs consistently arose

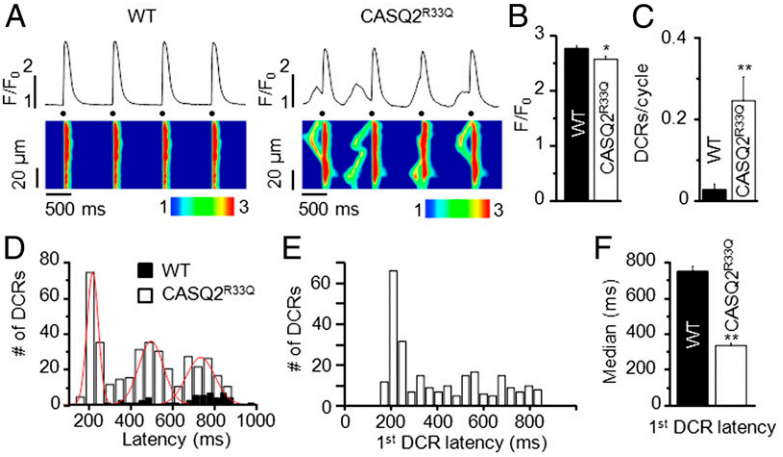

Fig. 1. Frequency and timing of spontaneous Ca^{2+} release in $CASQ2^{R33Q}$ isolated ventricular myocytes. (*A*) Representative line-scan images of WT and $CASQ2^{R33Q}$ isolated cardiomyocytes paced at 1 Hz (dots) in the presence of ISO (100 nM) show increased incidence of DCR events in $CASQ2^{R33Q}$ cells. (*B*) Stimulated Ca^{2+} transient amplitude in $CASQ2^{R33Q}$ and WT myocytes paced at 2 Hz in the presence of 100 nM ISO. F/F_0 (in which F is the fluorescence at time t and F_0 represents the background signal) is 2.56 ± 0.06 vs. 2.75 ± 0.06, respectively. Summary of DCR frequency (*C*) and DCR temporal distribution (*D*): DCRs are more common in $CASQ2^{R33Q}$ myocytes and occur at three distinct time points (interrelease latencies 337, 259, and 269 ms, respectively). (*E*) Distribution of the latency to the first DCR following a delay displays a prominent early peak. (*F*) The median of the first DCR latency occurs earlier in $CASQ2^{R33Q}$ cells relative to WT. (*B*) n = 24 and 10 cells for $CASQ2^{R33Q}$ and WT, respectively; (*C–F*) n = 59 and 30 cells for $CASQ2^{R33Q}$ and WT from five and three animals, respectively. *$P < 0.05$; **$P < 0.01$.

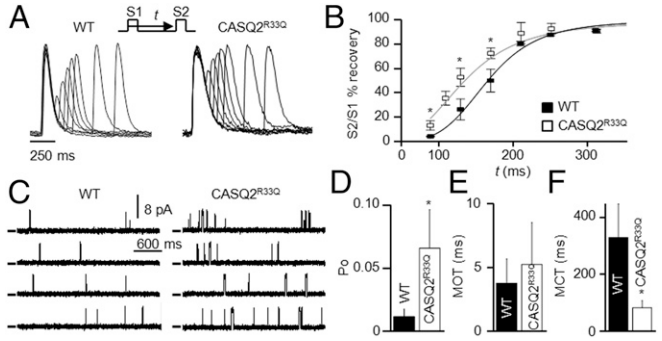

Fig. 2. Abbreviated RyR2 refractoriness underlies spontaneous Ca^{2+} release: single myocytes and single RyR2 channels experiments. (*A*) Representative traces of SR Ca^{2+} release attained during an S1-S2 restitution protocol show faster release recovery in $CASQ2^{R33Q}$ cardiomyocytes. Experiments were carried out in the presence of 100 nM ISO. (*B*) Average time course of the restitution of Ca^{2+} transients shows faster recovery of SR Ca^{2+} release in $CASQ2^{R33Q}$ myocytes relative to WT cells (time to half-maximal recovery was 134 ± 5 vs. 166 ± 2 ms respectively, $P < 0.001$). Each data point was recorded in 12–29 $CASQ2^{R33Q}$ and 6–11 WT myocytes, respectively. Restitution of Ca^{2+} transients in each group was fitted to logistic functions. (*C*) Sample recordings of RyR2 channels obtained from cardiac SR microsomes of WT and $CASQ2^{R33Q}$ mice. Open events are shown as upward deflections from the marked zero current level. $CASQ2^{R33Q}$ single RyR2s were more active. Bar graphs showing the Po (*D*), mean open time (MOT) (*E*), and MCT (*F*) of 8 WT and 4 $CASQ2^{R33Q}$ RyR2 channels. Single RyR2 Po was significantly greater and MCT significantly smaller in $CASQ2^{R33Q}$ mice compared with WT mice in a one-tail unpaired Student *t* test. $*P < 0.05$; $**P < 0.01$.

around three different diastolic time points as illustrated in Fig. 3*C*. These results suggest that DCs result from highly synchronized cellular events consistent with the temporal alignment of DCR observed in isolated myocytes.

To further assess the cellular synchronicity underlying the observed DCs, we examined the amplitude and decay rate of developed force during stimulated and spontaneous Ca^{2+} release (Fig. 3 *E* and *F*). Stimulated contraction (SC) of myocardium is maximally synchronized by electrical stimulus. Thus, we compared the amplitude and decay rate of DCs with SCs to determine the intrinsic synchronicity of the DCs. As demonstrated in Fig. 3*D*, a significant pool of DCs was similar in size or was even higher than SCs. Taken together, this suggests that most DCs recruited the vast majority of muscle cells and were likely associated with an ectopic AP.

DCR Is Synchronized in Intact $CASQ2^{R33Q}$ Cardiac Muscle. To directly examine synchronization of DCR between different myocytes in myocardium of $CASQ2^{R33Q}$ mice, we performed confocal Ca^{2+} imaging in cardiac muscle preparations. Muscles loaded with the cytosolic Ca^{2+} indicator Rhod-2 were paced at 1 Hz in the presence of ISO (Fig. 4). Consistent with the results in isolated myocytes, DCR in the form of Ca^{2+} waves occurred regularly between pacing-induced Ca^{2+} transients in the vast majority of $CASQ2^{R33Q}$ cells within the field of view (Fig. 4 *B* and *C*) but not in WT muscles (Fig. 4*A*). Once again, when we examined the timing of cellular DCRs within cardiac muscles, we observed three distinct time peaks similar to those observed in isolated myocytes (Fig. 4*D*). As in isolated myocytes, the distribution of DCRs and DCs in cardiac muscles was rate-dependent (Fig. S3). Furthermore, similar to the results of force measurements, the amplitudes of DCRs from a significant portion of myocytes were similar to those of Ca^{2+} transients generated by electrical stimulation (Fig. 4*E*).

Experiments conducted in isolated myocytes suggest that the temporal alignment of DCR arises from the shortened RyR2 refractory period following temporally uniform stimulated Ca^{2+} release and the resultant synchronized reuptake. To test the role of the stimulated Ca^{2+} release/reuptake in DCR synchronization, we examined the effects of a single electrical stimulation on the timing of DCR (Fig. 5*A*, *Left*). At rest, the muscles exhibited occasional Ca^{2+} waves that randomly occurred in different myocytes. Following an electrically induced Ca^{2+} transient, several sequential oscillations of Ca^{2+} release occurred in multiple adjacent cells, which gradually decreased in amplitude and in the degree of cohesiveness (Fig. 5*B*). Application of additional electrical stimuli once again resynchronized the diastolic release (Fig. 5*A*, *Right*). To quantify the degree of synchronicity of DCR, we measured the time interval (i.e., latency) to the first DCR following stimulated Ca^{2+} release and the time intervals between consecutive DCRs (Fig. 5*C*). The first DCR evidenced the shortest mean latency and smallest corresponding standard deviation (SD), suggesting the highest level of synchronicity. The subsequent DCRs evidenced longer latencies that were coupled to a greater variance in their occurrence. These results suggest that temporally uniform stimulated Ca^{2+} release/reuptake dynamics plays a key role in synchronization of DCR in $CASQ2^{R33Q}$ muscle. Of note, Ca^{2+} waves are capable of crossing cell boundaries apparently via gap junctions (25). However, the rate of propagation of isolated Ca^{2+} waves (~50 μm/s) in our study in the absence of pacing seems too slow to account for the high synchronicity of release in the wake of a temporally aligned pacing-induced Ca^{2+} transient.

For spontaneous Ca^{2+} release to become proarrhythmic, it must cause an ectopic AP that triggers an arrhythmia. As mentioned previously, the high amplitude of DCs and that of DCR events in intact tissue suggest an accompanying muscle-wide triggered electrical depolarization (i.e., extrasystolic AP). To test directly whether synchronous DCR can result in extrasystolic electrical activity in $CASQ2^{R33Q}$ muscles, we performed simultaneous Ca^{2+} and membrane potential (MP) imaging. Muscles were dual-labeled with Rhod-2 and RH237 or di-4-ANBDQBS for simultaneous Ca^{2+} and MP measurements, respectively, and stimulated at

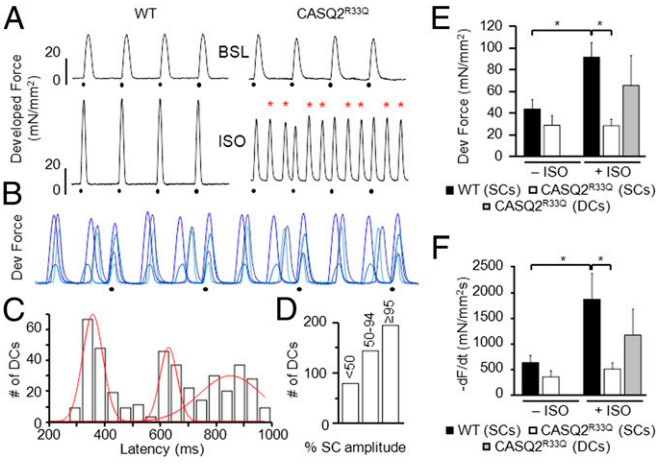

Fig. 3. $CASQ2^{R33Q}$ intact cardiac muscles show highly synchronized DCs. (*A*) Representative recordings of developed (Dev) force from WT and $CASQ2^{R33Q}$ cardiac muscles electrically stimulated at 1 Hz (dots). Superfusion with ISO (30–300 nM) resulted in DCs (red asterisks) in $CASQ2^{R33Q}$ but not in WT preparations. (*B*) Superimposed twitch recordings from four $CASQ2^{R33Q}$ muscles in the presence of ISO (30–300 nM) paced at 1 Hz (black dots) show that DCs consistently occur around the same time points (not to scale). (*C*) Cumulative temporal distribution of DCs in $CASQ2^{R33Q}$ muscles shows three probability peaks. (*D*) Distribution of DC amplitudes (as % of the mean value of the corresponding SC) in $CASQ2^{R33Q}$ muscles. Average amplitude (*E*) and decay rate (*F*) of WT and $CASQ2^{R33Q}$ contractions under baseline (BSL) conditions (– ISO) and under maximum effect of adrenergic stimulation (+ ISO, 30–300 nM). $n = 5$ muscles for both $CASQ2^{R33Q}$ and WT. $*P < 0.05$. –dF/dt, maximum of the first derivative of the developed force.

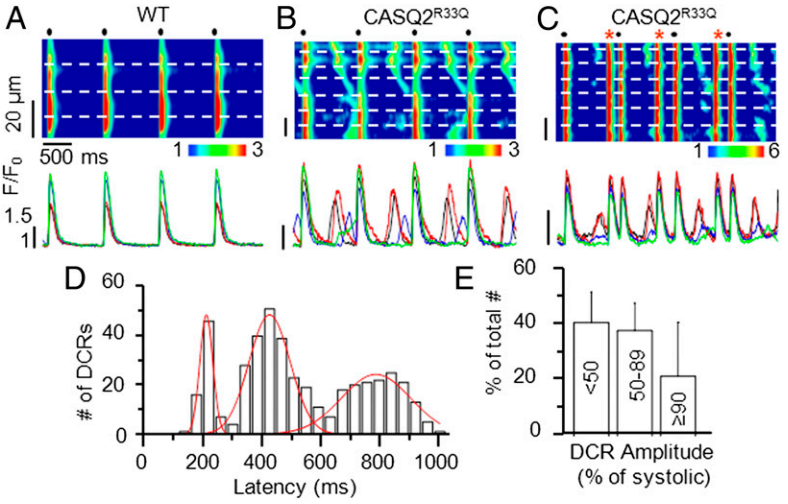

Fig. 4. Confocal Ca^{2+} imaging and timing of DCR in $CASQ2^{R33Q}$ intact cardiac muscles. Representative line-scan images of WT (*A*) and $CASQ2^{R33Q}$ (*B* and *C*) muscle preparations (*Upper*) along with fluorescence profiles from the top four myocytes within the tissue (*Lower*). Dashed white lines on the images show myocytes borders. Red asterisks indicate tissue-wide extrasystolic Ca^{2+} transients. Muscles were electrically stimulated at 1 Hz (black dots) in the presence of 100 nM ISO. (*D*) Temporal distribution of DCR in $CASQ2^{R33Q}$ muscles, showing three probability peaks. n = 21 cells from three preparations. (*E*) Distribution of DCR amplitudes (as % of the mean value of the corresponding stimulated Ca^{2+} transient) in myocytes from $CASQ2^{R33Q}$ muscles. n = 15 cells from three muscles.

1 Hz before and after infusion of ISO. Dual-labeled muscles evidenced an AP and a corresponding Ca^{2+} transient with each electrical stimulation (Fig. S4). Neither DCRs nor extrasystolic APs were detected in WT muscles, even in the presence of ISO (Fig. S4). On the other hand, we observed characteristic DCRs that were occasionally associated with extrasystolic APs in single myocytes (Fig. S5) as well as globally (Fig. 6 *A* and *B*) in ISO-treated $CASQ2^{R33Q}$ muscles. Overall, addition of ISO to $CASQ2^{R33Q}$ muscles resulted in a significant increase in the frequency of cellular DCRs and a corresponding rise in the rate of extrasystolic APs (Fig. 6*C*). The generation of cell-wide triggered activity is further substantiated by the similarity in the amplitudes of extrasystolic and electrically stimulated globally averaged AP signals (Fig. 6*D*). Taken together, these data suggest that aberrant SR Ca^{2+} release can indeed elicit a triggered arrhythmia in a cardiac muscle.

Last, we explored whether stabilization of the release machinery can potentially reverse the proarrhythmic spontaneous Ca^{2+} release events. Recent studies have shown that the muscle relaxant dantrolene may normalize abnormal Ca^{2+} handling associated with heart failure and CPVT by stabilizing the interdomain interactions within the RyR2 and by increasing the threshold for spontaneous Ca^{2+} release in cardiac myocytes (26, 27). The confocal line-scan images in a $CASQ2^{R33Q}$ cardiac muscle in Fig. 7*A* reveal that addition of dantrolene (+ Da) reduced DCR relative to ISO alone. Notably, the tissue-wide extrasystolic Ca^{2+} transients characteristic of $CASQ2^{R33Q}$ (Fig. 7*A*) were virtually absent following dantrolene exposure. Desynchronization of DCR by dantrolene is further illustrated by increased width of distribution (Fig. 7*B*) as well as prolonged time to the median (Fig. 7*C*) of the first DCR latency in dantrolene-treated muscles. Additionally, dantrolene significantly reduced the frequency of DCR (from 4 to 2.45 per cycle) and the amplitude of the first DCR (Fig. 7*D*). Thus, stabilization of RyR2 by dantrolene indeed alleviated aberrant Ca^{2+} cycling in $CASQ2^{R33Q}$ muscle.

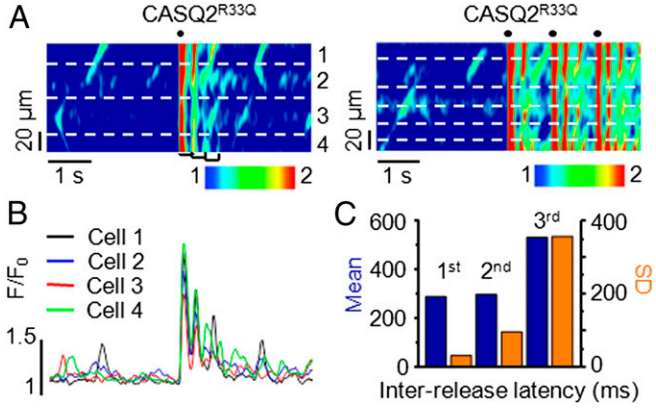

Fig. 5. High degree of DCR synchronicity in $CASQ2^{R33Q}$ intact cardiac muscles. (*A*) Line-scan images of a $CASQ2^{R33Q}$ muscle challenged with 100 nM ISO and 10 mM $[Ca^{2+}]_o$, showing DCR timing properties at rest and after a single electrical stimulation (*Left*) or a train of three stimuli (*Right*). (*B*) Fluorescence signals from each myocyte in the line-scan image of the $CASQ2^{R33Q}$ muscle shown in *A*, *Left*. (*C*) Mean and SD of the interrelease latencies for the first three Ca^{2+} oscillations as marked by the brackets in the line-scan image in *A*, *Left*. Data are representative of five experiments.

Discussion

In this study, we investigated the defective SR Ca^{2+} handling mechanisms that underlie triggered arrhythmias associated with CPVT on the molecular, cellular, and tissue levels. Our major finding is that DCR in the form of Ca^{2+} waves, commonly thought to result from spontaneous events in individual cells, occurs in a temporally and spatially uniform manner simultaneously in multiple cells across the myocardium of CPVT-susceptible mice. Such highly synchronized Ca^{2+} release events give rise to triggered electrical activity and synchronous DCs in intact cardiac muscle. Importantly, we determined that this coordinated, aberrant SR Ca^{2+} cycling is due to a combination of impaired refractory behavior of RyR2 channels and synchronous stimulated Ca^{2+} release/reuptake dynamics. Our study reveals how DCRs can be synchronized in the myocardium and lead to triggered activity in the setting of a cardiac rhythm disorder.

Synchronicity of DCR and DC in Cardiac Muscle. In this study, we focus on arrhythmogenesis associated with CPVT resulting from a defect in SR Ca^{2+} handling caused by a point-mutation (R33Q) in the SR Ca^{2+}-binding protein, CASQ2 (22, 24, 28). Previous studies showed that this and other CASQ2 mutations compromise RyR2 regulation by luminal Ca^{2+}, thereby causing DCR and DADs in cardiomyocytes (29–31). However, the precise mechanisms as well as the mode(s) of action through which such impaired myocyte Ca^{2+} handling on the cellular level leads to CPVT and other forms of Ca^{2+}-dependent arrhythmias in intact tissue remain to be defined. Here, we show that DCR in $CASQ2^{R33Q}$ myocytes occurs in a highly temporally uniform manner with a robust probability, which peaks around 200 ms after stimulated Ca^{2+} release (Fig. 1 *E* and *F*). This temporal alignment of DCR could provide a basis for synchronization of proarrhythmic Ca^{2+} signaling in the myocardium, as noted previously by Stern et al. (32). We directly confirmed this notion by using measurements of contractile force as well as

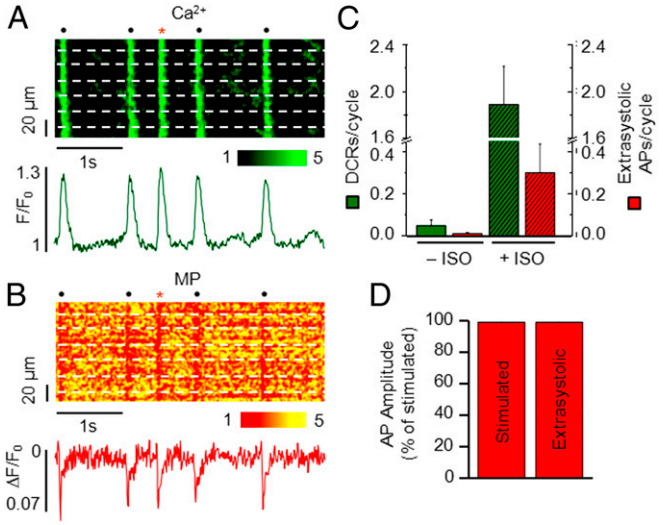

Fig. 6. Simultaneous recording of Ca^{2+} and MP signals in $CASQ2^{R33Q}$ cardiac muscle. (*A* and *B*) Confocal line-scan images of a $CASQ2^{R33Q}$ cardiac muscle simultaneously loaded with Rhod-2 (*A*) and di-4-ANBDQBS (*B*). Fluorescence signals of cytosolic Ca^{2+} and MP summated from the raw signals from all cells are shown below the line-scan images. The red asterisk indicates the extrasystolic beat. (*C*) Number of DCRs and extrasystolic APs per cycle with and without ISO. n = 6–21 cells. (*D*) Amplitude of the averaged stimulated AP and extrasystolic (unstimulated) AP. Data obtained from six muscles.

imaging of the intracellular Ca^{2+} and MP in electrically paced ventricular muscles. These studies revealed that indeed both DCRs and DCs occurred in a highly regular manner in $CASQ2^{R33Q}$, but appeared to be random in WT muscles (Fig. 3 *B* and *C*). Importantly, the stabilization of the Ca^{2+} release machinery with dantrolene improved regulation of Ca^{2+} cycling (27) and ameliorated the CPVT phenotype in our model. Of note, most DCs had amplitude and duration characteristics similar to those of contractions elicited by electrical stimulation. This suggests that, similar to SCs, most DCs involved rapid depolarization of many cells within the tissue and were likely associated with an ectopic AP (Fig. 3*D*). This assertion was directly confirmed by monitoring intracellular Ca^{2+} and MP in the muscle preparation with confocal microscopy. These experiments revealed that synchronization of DCR in adjacent myocytes was actually able to elicit triggered activity (Fig. 6). Taken together, these data demonstrate the capacity of DCR to synchronize in ventricular muscle and thereby elicit ectopic activity.

Mechanism of Synchronization of DCR. Based on our findings and results of previous studies (33–36), the mechanism of DCR synchronization in $CASQ2^{R33Q}$ myocardium depends on the efficiency of store-dependent RyR2 deactivation. In normal myocytes, reduction of luminal Ca^{2+} following release prompts RyR2s to deactivate via CASQ2, thereby rendering SR release refractory to spontaneous reactivation (7). In addition, depletion of SR Ca^{2+} content can facilitate release refractoriness by reducing Ca^{2+} efflux via RyR2s, thus interrupting local CICR signaling (6). In the $CASQ2^{R33Q}$ muscle, on the other hand, store-dependent RyR2 deactivation is compromised due to impaired RyR2 regulation by CASQ2, thus leaving SR release vulnerable to spontaneous reactivation (15, 37). In this study, we show that periodic DCR in $CASQ2^{R33Q}$ myocytes is associated with impaired Ca^{2+} signaling refractoriness, indicated by both shortened restitution of SR Ca^{2+} release and increased single RyR2 activity at diastolic luminal Ca^{2+} (Fig. 2). As suggested by Maltsev et al. (23), impaired Ca^{2+} signaling refractoriness increases the propensity of release sites to fire more synchronously by facilitating CICR and local recruitment of neighboring sites. This results in a transition of spontaneous local release events to global waves in cells prone to Ca^{2+} oscillations. Moreover, the prolongation of Ca^{2+} release refractoriness by dantrolene significantly reduces the probability of the aforementioned release sites to fire synchronously, reducing the proarrhythmic wave burden. Another critical factor in synchronization of DCR revealed here is the temporal uniformity introduced by electrically stimulated Ca^{2+} release and reuptake across the myocardium. Thus, impaired refractoriness along with synchronized SR Ca^{2+} reuptake provides a dynamic substrate for self-regenerating CICR.

Relation to Previous Studies. Our results are consistent with and expand on previous findings obtained from a postmyocardial infarction canine model of arrhythmia (31) that showed impaired Ca^{2+} store-dependent deactivation and compromised Ca^{2+} release refractoriness in isolated myocytes (33). Our findings are supported by experiments in whole hearts of $CASQ2^{-/-}$ mice that evidenced shortened Ca^{2+} release restitution (37). Furthermore, it has been previously reported that the time course of SR Ca^{2+} load influences the timing of spontaneous Ca^{2+} release in rat hearts (38), consistent with our current findings. In this previous study, however, SR Ca^{2+} release was only mildly synchronous because of the apparently largely preserved refractory behavior of SR Ca^{2+} release of normal rat hearts. This in part may explain why the arrhythmogenic potential of synchronized spontaneous SR Ca^{2+} release was not fully revealed as demonstrated here. Last, in accord with reports obtained from myocytes isolated from CPVT mouse (26) and failing rabbit hearts (27), we demonstrate that synchronized spontaneous SR Ca^{2+} release can be disrupted by

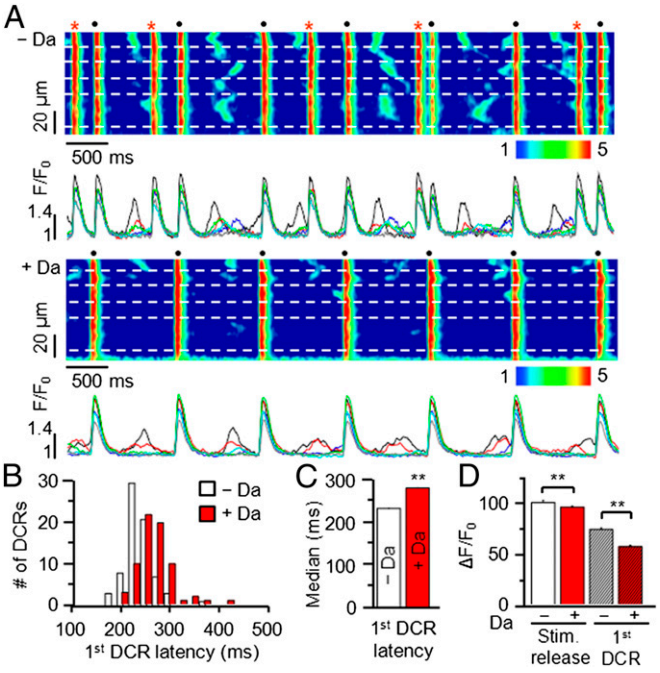

Fig. 7. RyR2 inhibitor dantrolene hampers simultaneous DCR in $CASQ2^{R33Q}$ cardiac muscle. (*A*) Confocal line-scan images of a $CASQ2^{R33Q}$ cardiac muscle before (– Da) and after (+ Da) exposure to 30 μM dantrolene for 30 min. Superimposed fluorescence profiles from the individual cells shown below the corresponding line-scans highlight the synchronization of DCR over time (– Da) or the lack thereof after treatment with dantrolene (+ Da). (*B*) Distribution of the latency to the first DCR before and after treatment with 30 μM dantrolene for 30 min. (*C*) Dantrolene significantly prolonged the median to the first DCR in $CASQ2^{R33Q}$ myocardium. (*D*) Dantrolene also significantly reduced the amplitude of the first DCR. Experiments were performed in the presence of 100 nM ISO, 3 mM $[Ca^{2+}]_o$, n = 70 DCRs from three muscles, $^{**}P < 0.01$. Stim, stimulated.

pharmacological stabilization of the RyR2 complex and subsequent prolongation of SR Ca^{2+} release refractoriness.

Summary. We show that impaired Ca^{2+} release refractoriness combined with uniform SR Ca^{2+} release in intact cardiac muscle synchronizes the DCR that underlies triggered arrhythmias in CPVT. These aberrant DCRs can be mitigated by pharmacological stabilization of the release machinery that improves abnormally abbreviated SR Ca^{2+} release refractoriness. It remains to be determined whether, and to what extent, such synchronization of Ca^{2+} release in ventricular myocardium as opposed to other tissue types (i.e., Purkinje fibers) contributes to clinically relevant arrhythmic episodes in CPVT and other forms of Ca^{2+}-dependent arrhythmias in the intact heart. Targeting DCR synchronization through reagents affecting RyR2 refractory behavior such as dantrolene may be an innovative strategy for development of mechanism-based antiarrhythmia therapies.

Materials and Methods

All animal procedures were approved by The Ohio State University Institutional Animal Care and Use Committee and conformed to the Guide for the Care and Use of Laboratory Animals published by the US National Institutes of Health [(NIH) Publication No. 85-23, revised 1996], and by the Animal Care and Use Committee of the University of Padova. Ventricular myocytes were obtained by enzymatic isolation as previously described (39). I_{Ca} were recorded using whole-cell patch-clamp technique. Fluo-3 (an intracellular Ca^{2+} indicator) fluorescence was recorded in the line scan mode of the confocal microscope. SR microsomes were prepared from homogenized WT and $CASQ2^{R33Q}$ mouse ventricular muscle, and single channels were recorded as previously described (24). Trabeculae or papillary muscles were used for force measurement as described previously (40). For confocal Ca^{2+} and MP imaging, muscles were loaded with the cytosolic Ca^{2+} indicator Rhod-2 AM (40 μM). For some experiments, the muscles were also stained with MP indicator RH237 or di-4-ANBDQBS (Richard D. Berlin Center for Cell Analysis and Modeling, University of Connecticut Health Center). Detailed material and methods can be found in *SI Materials and Methods*.

ACKNOWLEDGMENTS. This work was supported by NIH Grants HL074045 and HL063043 (to S.G.), NIH Grants HL07832 and AR054098 (to M.F.), and Italian Telethon Organizzazione Non Lucrativa di Utilità Sociale (ONLUS) Foundation Grant GGP11141 and Fondazione Cassa di Risparmio delle Provincie Lombarde (Cariplo) Grant p2008.2275 (to P.V.). L.B. is supported by the Great Rivers Affiliate, American Heart Association Postdoctoral Fellowship 13POST14050001.

1. Roger VL, et al.; American Heart Association Statistics Committee and Stroke Statistics Subcommittee (2012) Heart disease and stroke statistics—2012 update: A report from the American Heart Association. *Circulation* 125(1):e2–e220.
2. Bers DM (2001) *Excitation–Contraction Coupling and Cardiac Contractile Force* (Springer, Dordrecht), 2nd Ed.
3. Terentyev D, Viatchenko-Karpinski S, Valdivia HH, Escobar AL, Györke S (2002) Luminal Ca^{2+} controls termination and refractory behavior of Ca^{2+}-induced Ca^{2+} release in cardiac myocytes. *Circ Res* 91(5):414–420.
4. Szentesi P, Pignier C, Egger M, Kranias EG, Niggli E (2004) Sarcoplasmic reticulum Ca^{2+} refilling controls recovery from Ca^{2+}-induced Ca^{2+} release refractoriness in heart muscle. *Circ Res* 95(8):807–813.
5. Sobie EA, Song L-S, Lederer WJ (2005) Local recovery of Ca^{2+} release in rat ventricular myocytes. *J Physiol* 565(Pt 2):441–447.
6. Guo T, Gillespie D, Fill M (2012) Ryanodine receptor current amplitude controls Ca^{2+} sparks in cardiac muscle. *Circ Res* 111(1):28–36.
7. Györke S, Terentyev D (2008) Modulation of ryanodine receptor by luminal calcium and accessory proteins in health and cardiac disease. *Cardiovasc Res* 77(2):245–255.
8. Qin J, et al. (2008) Luminal Ca^{2+} regulation of single cardiac ryanodine receptors: Insights provided by calsequestrin and its mutants. *J Gen Physiol* 131(4):325–334.
9. Györke I, Hester N, Jones LR, Györke S (2004) The role of calsequestrin, triadin, and junctin in conferring cardiac ryanodine receptor responsiveness to luminal calcium. *Biophys J* 86(4):2121–2128.
10. Ter Keurs HEDJ, Boyden PA (2007) Calcium and arrhythmogenesis. *Physiol Rev* 87(2): 457–506.
11. Laurita KR, Rosenbaum DS (2008) Mechanisms and potential therapeutic targets for ventricular arrhythmias associated with impaired cardiac calcium cycling. *J Mol Cell Cardiol* 44(1):31–43.
12. Weiss JN, Nivala M, Garfinkel A, Qu Z (2011) Alternans and arrhythmias: From cell to heart. *Circ Res* 108(1):98–112.
13. Venetucci LA, Trafford AW, O'Neill SC, Eisner DA (2008) The sarcoplasmic reticulum and arrhythmogenic calcium release. *Cardiovasc Res* 77(2):285–292.
14. Györke S, Carnes C (2008) Dysregulated sarcoplasmic reticulum calcium release: Potential pharmacological target in cardiac disease. *Pharmacol Ther* 119(3):340–354.
15. Györke S (2009) Molecular basis of catecholaminergic polymorphic ventricular tachycardia. *Heart Rhythm* 6(1):123–129.
16. Napolitano C, Priori SG (2007) Diagnosis and treatment of catecholaminergic polymorphic ventricular tachycardia. *Heart Rhythm* 4(5):675–678.
17. Lederer WJ, Tsien RW (1976) Transient inward current underlying arrhythmogenic effects of cardiotonic steroids in Purkinje fibres. *J Physiol* 263(2):73–100.
18. Radwański PB, Poelzing S (2011) NCX is an important determinant for premature ventricular activity in a drug-induced model of Andersen-Tawil syndrome. *Cardiovasc Res* 92(1):57–66.
19. Radwański PB, Veeraraghavan R, Poelzing S (2010) Cytosolic calcium accumulation and delayed repolarization associated with ventricular arrhythmias in a guinea pig model of Andersen-Tawil syndrome. *Heart Rhythm* 7(10):1428–1435.e1.
20. Xie Y, Sato D, Garfinkel A, Qu Z, Weiss JN (2010) So little source, so much sink: Requirements for afterdepolarizations to propagate in tissue. *Biophys J* 99(5): 1408–1415.
21. Herron TJ, Milstein ML, Anumonwo J, Priori SG, Jalife J (2010) Purkinje cell calcium dysregulation is the cellular mechanism that underlies catecholaminergic polymorphic ventricular tachycardia. *Heart Rhythm* 7(8):1122–1128.
22. Rizzi N, et al. (2008) Unexpected structural and functional consequences of the R33Q homozygous mutation in cardiac calsequestrin: A complex arrhythmogenic cascade in a knock in mouse model. *Circ Res* 103(3):298–306.
23. Maltsev AV, et al. (2011) Synchronization of stochastic Ca^{2+} release units creates a rhythmic Ca^{2+} clock in cardiac pacemaker cells. *Biophys J* 100(2):271–283.
24. Terentyev D, et al. (2008) Modulation of SR Ca release by luminal Ca and calsequestrin in cardiac myocytes: Effects of CASQ2 mutations linked to sudden cardiac death. *Biophys J* 95(4):2037–2048.
25. Lamont C, Luther PW, Balke CW, Wier WG (1998) Intercellular Ca^{2+} waves in rat heart muscle. *J Physiol* 512(Pt 3):669–676.
26. Kobayashi S, et al. (2010) Dantrolene, a therapeutic agent for malignant hyperthermia, inhibits catecholaminergic polymorphic ventricular tachycardia in a RyR2 (R2474S/+) knock-in mouse model. *Circ J* 74(12):2579–2584.
27. Maxwell JT, Domeier TL, Blatter LA (2012) Dantrolene prevents arrhythmogenic Ca^{2+} release in heart failure. *Am J Physiol Heart Circ Physiol* 302(4):H953–H963.
28. Terentyev D, et al. (2006) Abnormal interactions of calsequestrin with the ryanodine receptor calcium release channel complex linked to exercise-induced sudden cardiac death. *Circ Res* 98(9):1151–1158.
29. di Barletta MR, et al. (2006) Clinical phenotype and functional characterization of CASQ2 mutations associated with catecholaminergic polymorphic ventricular tachycardia. *Circulation* 114(10):1012–1019.
30. Terentyev D, et al. (2003) Calsequestrin determines the functional size and stability of cardiac intracellular calcium stores: Mechanism for hereditary arrhythmia. *Proc Natl Acad Sci USA* 100(20):11759–11764.
31. Knollmann BC, et al. (2006) Casq2 deletion causes sarcoplasmic reticulum volume increase, premature Ca^{2+} release, and catecholaminergic polymorphic ventricular tachycardia. *J Clin Invest* 116(9):2510–2520.
32. Stern MD, Kort AA, Bhatnagar GM, Lakatta EG (1983) Scattered-light intensity fluctuations in diastolic rat cardiac muscle caused by spontaneous Ca++-dependent cellular mechanical oscillations. *J Gen Physiol* 82(1):119–153.
33. Radwański PB, Belevych AE, Brunello L, Carnes CA, Györke S (2013) Store-dependent deactivation: Cooling the chain-reaction of myocardial calcium signaling. *J Mol Cell Cardiol* 58:77–83.
34. Belevych AE, et al. (2011) The relationship between arrhythmogenesis and impaired contractility in heart failure: Role of altered ryanodine receptor function. *Cardiovasc Res* 90(3):493–502.
35. Ramay HR, Liu OZ, Sobie EA (2011) Recovery of cardiac calcium release is controlled by sarcoplasmic reticulum refilling and ryanodine receptor sensitivity. *Cardiovasc Res* 91(4):598–605.
36. Belevych AE, et al. (2012) Shortened Ca^{2+} signaling refractoriness underlies cellular arrhythmogenesis in a postinfarction model of sudden cardiac death. *Circ Res* 110(4): 569–577.
37. Kornyeyev D, et al. (2012) Calsequestrin 2 deletion shortens the refractoriness of Ca^{2+} release and reduces rate-dependent Ca^{2+}-alternans in intact mouse hearts. *J Mol Cell Cardiol* 52(1):21–31.
38. Wasserstrom JA, et al. (2010) Variability in timing of spontaneous calcium release in the intact rat heart is determined by the time course of sarcoplasmic reticulum calcium load. *Circ Res* 107(9):1117–1126.
39. Zhao W, et al. (2003) Combined phospholamban ablation and SERCA1a overexpression result in a new hyperdynamic cardiac state. *Cardiovasc Res* 57(1):71–81.
40. Hiranandani N, Bupha-Intr T, Janssen PML (2006) SERCA overexpression reduces hydroxyl radical injury in murine myocardium. *Am J Physiol Heart Circ Physiol* 291(6): H3130–H3135.